Chest Tomography by Gamma Camera and External Gamma Source: Concise Communication

Massimo Pistolesi, Stefano Solfanelli, Riccardo Guzzardi, Maurizio Mey, and Carlo Giuntini

National Research Council Clinical Physiology Laboratory and 2nd Medical Clinic of the University of Pisa, Pisa, Italy

To obtain tomographic images of the chest, we used a large-field gamma camera to detect the 90° scattered radiations (180 keV) from a linear source of Hg-203 (279 keV). The primary beam traveling across the chest is scattered according to the relative density of tissues. Chest sections can be visualized at different depths on frontal and sagittal planes. The resolution of the technic is that of the gamma camera.

J Nucl Med 19: 94–97, 1978

Chest radiographic tomography has been widely used in clinical practice to obtain information about selected planes parallel or orthogonal to a frontal section of the body (*1–3*). Its advantages and limits are well known.

Tomographic images of a radioactive tracer's distribution in the chest may be obtained in various ways. One approach follows the principle of x-ray tomography, giving a longitudinal section, parallel to the frontal plane of the body, with the neighbouring sections blurred by relative motion (*4–8*).

A second approach is based on positron emission with coincidence detection. Positron-emission tomography permits the visualization of transverse chest sections by mathematical reconstruction of data from coincidence detectors mounted in a rotating array (*9*). Positron cameras using Anger's twin crystals (*10*) and the Massachusetts General Hospital's multiple crystals (*11,12*) give tomographic sections of the chest without relative motion between subject and detectors. All these methods, however, are either exceedingly complex or have poor tomographic resolution.

Computerized axial tomography provides images of transverse planes of the chest by measuring relative x-ray absorption. Tomograms obtained in this way (*13–16*) have the best anatomic resolution, but may represent only transverse chest sections and require a significant radiation dose.

Technics based on Compton scattering (*17–21*) either aim to measure absolute density of a small element of lung volume (*19,20*), or employ detecting devices other than a gamma camera and do not yield images comparable to those we are presenting (*17, 18,21*).

The aim of this paper is to describe a new method that permits the visualization of frontal and sagittal planes of the chest according to their density. Sectional visualization of the chest is obtained by employing a linear source of gamma photons and an imaging device—e.g., a gamma camera—to detect the Compton scattering at 90° to the primary beam.

MATERIALS AND METHODS

The gamma source is Hg-203. Its monoenergetic emission at 279 keV is in the range where, for interaction with materials such as human tissues, Compton effect is one order of magnitude greater than photoelectric effect. Furthermore, the energy of the 90° scattered photons (180 keV) is favorable for detection with imaging devices such as a gamma camera. Finally, the emitter's physical half-life (46.9 days) is long enough to enable the use of the source for 2–3 mo, when the initial activity is about one curie.

Received May 11, 1977; revision accepted Aug. 12, 1977.

For reprints contact: Carlo Giuntini, Laboratory of Clinical Physiology and Second Medical Clinic, University of Pisa, Pisa, Italy.

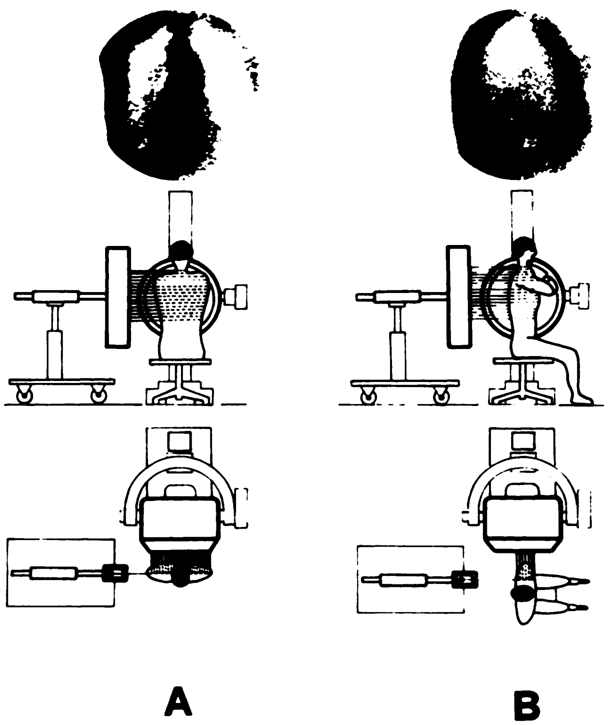

FIG. 1. Schematic representation of external gamma source and gamma camera. (A) Positioning of patient for frontal chest tomogram; (B) positioning for sagittal tomogram.

The Hg-203 source, in a glass tube 80 cm long, is enclosed in a lead box except for a slit 3 mm wide (Fig. 1). The primary beam, traveling across the chest, is scattered according to tissue density. The 90° scattered radiations are recorded by a large-field gamma camera and anatomic cross-sections of the chest can be visualized at different depths on the frontal (Fig. 1 A) and the sagittal (Fig. 1 B) planes. To permit chest imaging also in the supine position, the linear source can be wheeled around, moved up and down, and rotated.

The energy selector of the camera, set on 180 keV (window 15%), and an appropriate high-energy collimator (usable up to 410 keV) maximize detection of scattering events to those near 90°. With this setup, frontal tomograms with 400,000 counts are obtained in 3–5 min. Sagittal tomograms with 300,000 counts are obtained in somewhat shorter time.

Following the calculations developed by Lale (*17*) we estimate an absorbed dose of 0.09 rads for each view as a maximum estimate. Since sternal and vertebral bone marrow is usually not irradiated by the primary beam, its absorbed dose is less than with radiographic technics.

The resolution of the technic was tested on a phantom of the human chest. The chest wall was simulated by perspex slices 2.5 cm thick and the lung by a box filled with sawdust of 0.2 g/cc. A wooden frame of 0.4 density with paired holes of different diameters was put inside the box. The technic resolved holes 10 mm in diameter.

Geometry of the primary beam in air was studied by autoradiography at various film-to-lead-box distances. The beam's spread on the film was measured by an optical densitometer and the spread function plotted as optical density at each distance. At 30 cm from the lead box, the beam spread (FWHM) was about twice that at 7 cm.

CLINICAL APPLICATIONS

Three clinical examples will illustrate the ability of the technic to give a density image of any selected longitudinal plane of the chest.

The first series of pictures (Fig. 2) is from a patient with diffuse pulmonary emphysema. The frontal tomograms (Fig. 2 A,B,C) demonstrate the

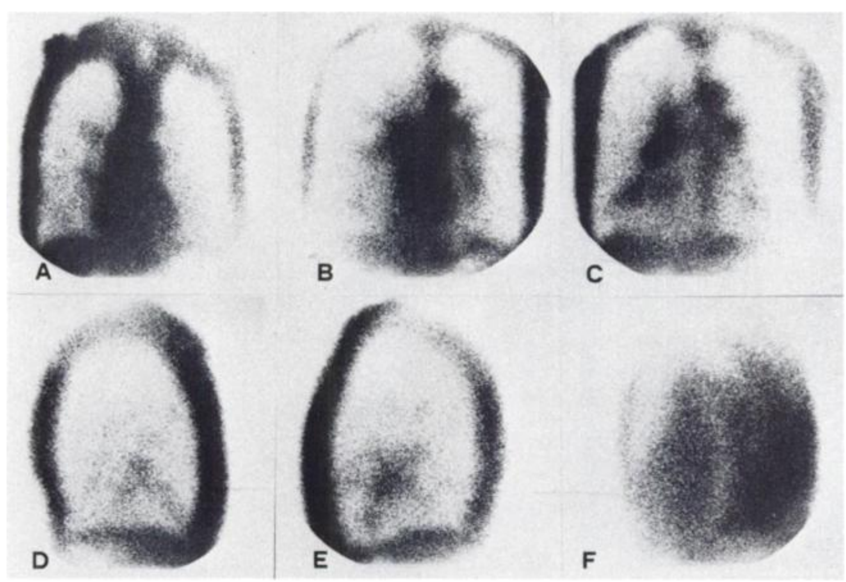

FIG. 2. (A,B,C) Frontal chest tomograms from a patient with emphysema, taken with primary beam incident on the anterior, middle, and posterior axillary lines. (D,E,F) Sagittal tomograms taken with primary beam incident on right and left mid hemithoraces and on the spine. All views demonstrate markedly reduced and nonhomogeneous lung density.

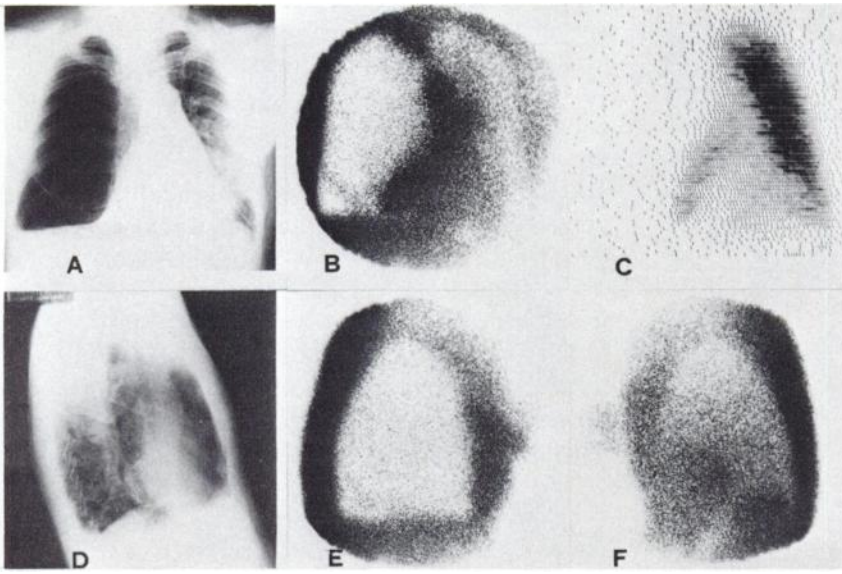

FIG. 3. (A) Frontal chest radiograph of patient with right pneumothorax. (B) Frontal tomograms showing the marked density difference between the two hemithoraces. (C) Frontal perfusion scan indicating a region of perfusion along right border of heart; it corresponds to a protruding density seen in frontal tomogram but not in chest x-ray. (D) Lateral chest radiograph. (E,F) Sagittal tomograms of right and left hemithoraces, with their marked difference in density and shape.

ability to visualize anatomic sections of the chest at different depths and to assess lung density. The mediastinal structures including the heart (Fig. 2 A), the hila (Fig. 2 B), and the major pulmonary vessels (Fig. 2 C), are clearly discernible. The sagittal tomograms (Fig. 2 D, E) sharply outline the lung tissue with respect to the chest wall. Starting from a mediastinal plane (Fig. 2 F) each lung may be divided into a number of sections in order to obtain detailed information about pathologic processes that alter the tissue density diffusely or focally.

In the second patient (Fig. 3), with a right-sided pneumothorax due to rupture of emphysematous bullae, the striking difference between the two hemithoraces is visualized by the 90° scattering tomograms in the frontal and sagittal planes. The chest radiograph fails to show any density in the region of the collapsed right lung, since the right cardiac border looks bare (Fig. 3 A). The frontal tomogram, by contrast (Fig. 3 B), clearly shows a density in that area protruding into the right hemithorax. The perfusion scan, obtained after i.v. injection of human albumin macroaggregates labeled with I-131, shows that this border corresponds to the outer limit of the collapsed right lung (Fig. 3 C). Failure of roentgenograms to visualize the collapsed lung can be ascribed to lack of absorption in the vacated space surrounding the collapsed lung tissue.

In the patient of Fig. 4, with proven chronic pulmonary tuberculosis, standard chest radiographs showed an increased density in the lower third of the left lung suspected to be neoplastic by clinicians

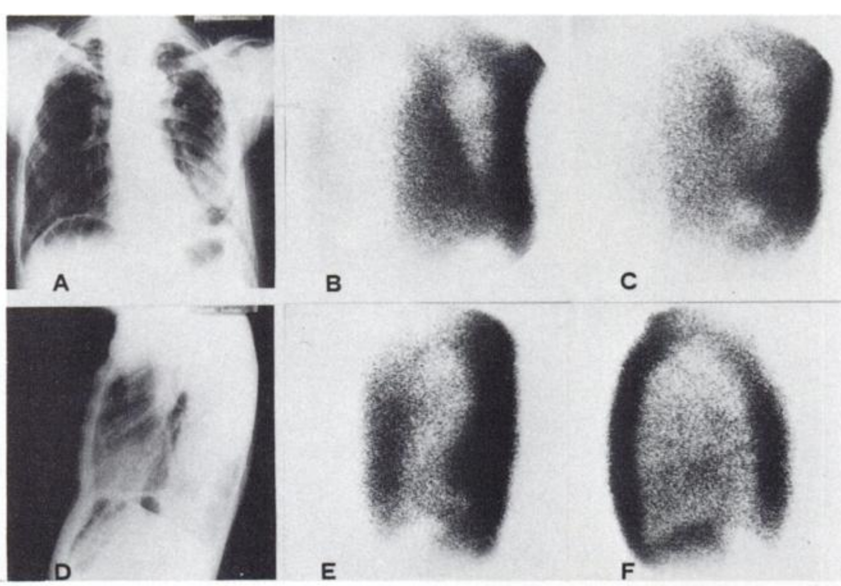

FIG. 4. (A) Frontal chest radiograph of a patient with old tuberculous lesions. Increased density in lower left lung field was suspected to be neoplastic. (B) Frontal tomogram taken with primary beam incident on anterior axillary line, showing reduced space between heart and chest wall. (C) Frontal tomogram with primary beam on posterior axillary line showing described increase in density. Aortic density is also clearly visible. (D) Lateral chest x-ray provides no further information on described density. (E) Sagittal tomogram of left lung reveals a density with sharp limits, contiguous with chest wall. It is apparently shaped by gravity, and can be interpreted as a circumscribed pleural effusion. (F) Sagittal tomogram of right lung.

and radiologists. Conventional x-ray tomography, as well as a lateral chest radiograph, assigned the density to the posterior region, but offered no further information. The 90° scattering tomograms, especially that in the sagittal view (Fig. 4 E), displayed the density and shape typical of pleural effusion.

DISCUSSION

The clinical applications of 90° Compton scattering tomography demonstrate the possibility of portraying changes in lung density caused by pathologic processes. Indeed, the lung presents ideal characteristics to be studied with this technic. Its gaseous components have a mass scattering coefficient for Hg-203 energy similar to that of lung tissue or other organic tissues, but the actual lung density, due to the physical presence of gas, reduces significantly the Compton scattering per unit area and helps to outline normal lung tissue in contrast to chest wall, mediastinum, and lung lesions.

One drawback is the attenuation of the primary beam in the tissues, which makes the image of structures fainter the farther they are from the source. Furthermore, autoradiography of the primary beam in air indicates a significant spreading of the beam with distance. Consequently, physical absorption in tissues and the fanning out of the primary beam lead to reduction of scattering events as one moves away from the source.

Given a known attenuation coefficient, physical absorption can be estimated from the image itself by an iterative procedure programmed on a digital computer on line with the camera. The geometric degradation of the beam may be eliminated by a more appropriate housing and collimation of the linear source.

Since, in frontal and sagittal chest tomograms, the paths of 90°-scattered photons are similar for each tomographic plane, their attenuation should be rather uniform. At any rate, attenuation differences may be dealt with by multiple-layer tomograms.

Contamination of the 90° scatter by multiple-scattered photons (*21*) is controlled by an 8-cm-thick, parallel-hole, collimator together with energy discrimination. With these expedients the large-field camera accepts less than 0.01% of all the scattered radiation. This could be further reduced if required. Model studies show that the index of resolution (FWHM) of the camera (*8*) corresponds to the size of the model holes that can be resolved.

Finally, 90° Compton scattering tomograms of the chest encompass larger sections than those obtained by roentgenograms and give images essentially without superposition of blurred structures, thus offering better density discrimination.

REFERENCES

1. ANDREWS RJ: Roentgenography: Body section. In *Medical Physics*, Glasser O, ed, Chicago, Year Book Publishers, 1955, pp 1264–1267

2. VALLEBONA A: Axial transverse laminagraphy. *Radiology* 55: 271–273, 1950

3. GREENE R: Fluoroscopic axialography: Clinical applications in thoracic disease. *Radiology* 121: 527–531, 1976

4. KUHL DE, EDWARDS RQ: Image separation radioisotope scanning. *Radiology* 80: 653–661, 1963

5. VOLPE JA, MCRAE J, ANGER HO: Clinical experience with the multiplane tomographic scanner. *J Nucl Med* 12: 101–106, 1971

6. MCAFEE JG, MOZLEY JM, STABLER EP: Longitudinal tomographic radioisotopic imaging with a scintillation camera: Theoretical considerations of a new method. *J Nucl Med* 10: 654–659, 1969

7. FREEDMAN GS: Tomography with a gamma camera. *J Nucl Med* 11: 602–604, 1970

8. MUEHLLEHNER G: A tomographic scintillation camera. *Phys Med Biol* 16: 87–96, 1971

9. TER-POGOSSIAN MM, PHELPS ME, HOFFMAN EJ, et al: A positron-emission transaxial tomograph for nuclear imaging (PETT). *Radiology* 114: 89–98, 1975

10. ANGER HO: Radioisotope cameras. In *Instrumentation in Nuclear Medicine,* vol. 1, Hine GJ, ed, New York, Academic Press, 1967, pp 485–550

11. BROWNELL GL, BURNHAM CA: Recent developments in positron scintigraphy. In *Instrumentation in Nuclear Medicine,* vol 2, Hine GJ, Sorenson JA, eds, New York, Academic Press, 1973, pp 135–159

12. CHESLER DA, HALES C, HNATOWICH DJ, et al: Three-dimensional reconstruction of lung perfusion image with positron detection. *J Nucl Med* 16: 80–82, 1975

13. SCHELLINGER D, DI CHIRO G, AXELBAUM SP, et al: Early clinical experience with the ACTA scanner. *Radiology* 114: 257–261, 1975

14. ALFIDI RJ, HAAGA J, MEANEY TF, et al: Computed tomography of the thorax and abdomen; a preliminary report. *Radiology* 117: 257–264, 1975

15. SAGEL S, STANLEY RJ, EVENS RG: Early clinical experience with motionless whole body computed tomography. *Radiology* 119: 321–330, 1976

16. SHEEDY II PF, STEPHENS DH, HATTERY RR, et al: Computed tomography of the body: initial clinical trial with the EMI prototype. *Am J Roentgenol Radium Ther Nucl Med* 127: 23–51, 1976

17. LALE PG: The examination of internal tissues, using gamma-ray scatter with a possible extension to megavoltage radiography. *Phys Med Biol* 4: 159–167, 1959

18. FARMER FT, COLLINS MP: A further appraisal of the Compton scattering method for determining anatomical cross-sections of the body. *Phys Med Biol* 19: 808–818, 1974

19. KAUFMAN L, GAMSU G, SAVOCA C, et al: Measurement of absolute lung density by Compton-scatter densitometry. *IEEE Trans Nucl Sci* 23: 599–605, 1976

20. GARNETT ES, WEBBER CE, COATES G, et al: Lung density: clinical method for quantitation of pulmonary congestion and edema. *CMA Journal* 116: 153–154, 1977

21. BATTISTA JJ, SANTON LW, BRONSKILL MJ: Compton scatter imaging of transverse sections: corrections for multiple scatter and attenuation. *Phys Med Biol* 22: 229–244, 1977